SEMARAK ILMU PUBLISHING

Journal of Advanced Research in Fluid Mechanics and Thermal Sciences

Journal homepage:
https://semarakilmu.com.my/journals/index.php/fluid_mechanics_thermal_sciences/index
ISSN: 2289-7879

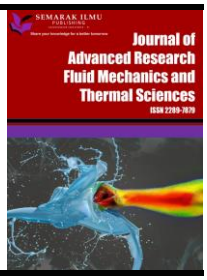

Effects of Hall Current and Activation Energy on a Three-Dimensional Rotating Casson Hybrid Nanofluid Flow over a Stretched Plate in the Presence of Joule Heating and Nonlinear Thermal Radiation

David Kumar[1,*], Bhagya Swetha Latha Kolapati[1], Rajasekhar Kandi[2]

[1] Department of Mathematics, Acharya Nagarjuna University, Guntur, AP, India
[2] Department of Mathematics, R.V.R. & J.C College of Engineering, Guntur, AP, India

ARTICLE INFO

Article history:
Received 9 June 2023
Received in revised form 11 August 2023
Accepted 22 August 2023
Available online 8 September 2023

Keywords:
Hybrid nanofluids; chemical reaction; stretching plate; rotation parameter; Hall current; boundary layer

ABSTRACT

The present study is related to the effects of activation energy and hall current on three-dimensional mixed convective casson hybrid Fe_3O_4/Al_2O_3 nanofluid rotating flow over-stretched plate in the presence of joule heating and nonlinear thermal radiation. The governing model of partial differential equations (PDE) is altered into ordinary differential equations (ODE) with an appropriate similarity transformation. The Numerical method which means shooting method based on the fourth-order Runge–Kutta method is applied to solve the system of nonlinear ODEs. Graphs and tables are used to study the impact of monitoring parameters on velocity, temperature, concentration profiles, reduced Nusselt number, reduced Sherwood numbers, and skin friction coefficients. Outstanding agreement is obtained when the present findings of the study is compared with the previous related research works. In the study, it is noted that an increase of the thermal radiation and activation energy parameters contributes to an increase of the flow temperature and concentration respected regions. The fluid velocity has enhanced with increasing values of hall parameters, whereas the opposite behavior has observed with increasing values of rotation parameter.

1. Introduction

Due to its wide range of applications in biomedicine, heat exchangers, cooling of electrical devices, double pane windows, food, transportation, etc., the concept of nanofluids have become a more widespread area of research for scientists in recent times. To enhance the thermal conductivity of base fluids such as ethylene glycol, water, kerosene, and motor oils, it is necessary to add nanoparticles such as graphene, silica, silver, gold, copper, alumina, carbon annotates, etc. The diameter of such nanoparticles may vary anywhere between 1-100 nm. It was Choi and Eastman [1] who first observed that nanoparticles suspended in base fluid could enhance the thermal conductivity which in turn improved the heat transfer rate of the fluid. Later, Buongiorno [2] investigated the factors that influenced the thermal conductivity of nanofluids and reported that

* *Corresponding author.*
E-mail address: davidparisa44@gmail.com

https://doi.org/10.37934/arfmts.109.1.5170

Brownian motion and thermophoresis effect increases the nanofluids thermal conductivity. As a consequence of the revelation, Nield and Kuznetsov [3] used the Buongiorno's model on the boundary layer stream. Khan and Pop [4] were the first to explore the steady flow of nanofluid on a stretching sheet using convective boundary conditions. Hamid *et al.,* [5] investigated the bio-convection flow of magneto-cross nanofluid including microorganisms by using an effective Prandtl number technique. Varun Kumar *et al.,* [6] explored the Arrhenius activation energy for hybrid nanofluid fluid above a curved stretching surface. Shah *et al.,* [7] used the Prandtl hybrid nanofluid flow with chemical reactions and motile microorganisms to study the bio-convection effects. Faraz *et al.,* [8] explored the multi-slip effect on axisymmetric Casson fluid flow with a chemical reaction. Arshad and Hassan [9] numerically investigated the hybrid nanofluid flow over permeable stretching surface considering magnetic field. Hassan *et al.,* [10] explored viscous dissipation and heat absorption with chemical reactions and heat source/sink. Krishnamurthy *et al.,* [11] explored the chemical reaction effects and melting heat transfer for frontier layer slip flow.

A new type of fluid, called a hybrid nanofluid, is finding widespread technological usage due to its excellent thermophysical properties. Hybrid nanofluids are the advanced fluid composed by adding two or more nanoparticles in a base fluid. Such kinds of nanofluids have more advanced properties than conventional nanofluids. An individual substance may never possess all of the needed traits; hence, the substance may be missing or deficient in some properties. Customizable hybrid nanoparticles can process important information more effectively than other nanofluids. Hybrid nanofluids ordinary outperform nanofluids in a variety of heat transfer applications, making them ideal for use in industries as diverse as refrigeration, electronics cooling, drug reduction, generator cooling, machining coolant, cooling for nuclear systems, cooling for transformers, biomedicine, and many more. Recently, Sundar *et al.,* [12] has suggested detailed procedure for creating hybrid nanofluids, including their benefits and drawbacks. Waini *et al.,* [13] have studied the unsteady flow of a hybrid nanofluid made by adding Cu nanoparticles in $Al2O3$ /water nanofluid due to a stretching/shrinking sheet. Lund *et al.,* [14] numerically computed the MHD hybrid nanofluid flow toward the shrinking surface for stability analysis and dual solutions and their problem consists of $Cu - Al_2O_3 -$ water the base fluid. They found that for increasing values of suction and radiation parameters temperature is enhanced (decrease) for both solutions. Shoaib *et al.,* [15] scrutinized the phenomena of viscous dissipation in 3D MHD hybrid nanofluid flow via rotating disk. In this research work, it is noted that magnetic field reduced both the radial and azimuthal skin frictions coefficients. Ahmad *et al.,* [16] pointed out the study of Go + Silver (Ag) in Maxwell hybrid nanoliquid for the improvement of thermal performance. Their concluding remarks illustrated that the heat transition is improved through the addition of silver volume fraction with graphene oxide. Alhussain and Tassaddiq [17] inspected the influence of variable viscosity in a blood-based two-dimensional Casson hybrid nanofluid through the stretching sheet by introducing a magnetic field perpendicular in a flow field. From this analysis, the authors have demonstrated that with the increment of nanomaterials concentration in the base fluid, the thermal expansion rate is increased but the specific heat capacity decreased.

Thermal radiation's effect on natural convection has risen in prominence due to its many practical applications in engineering and physics, especially in the development of tools and machinery, aerospace engineering, and gas turbines. Since it does not need a medium, thermal radiation is the preferred mode of heat transmission above conduction and convection. Because of these characteristics, thermal radiation plays a crucial role in the heat transmission of MHD nanofluids, minimising heat loss. Among the most important control elements for the flux of liquid and heat in a high-temperature heat system are radiation parameters. Thermal radiation has an essential impact on the development of steady kit, satellites, nuclear energy plants, turbines of gas, assortment of

advanced transformation systems and missiles. Elsaid and AlShurafat [18] have analyzed Impact of Hall Current and Joule Heating on a Rotating Hybrid Nanofluid Over a Stretched Plate with Nonlinear Thermal Radiation. In the early stage, the impact of heat radiation on Air and CO_2 of laminar flow through the vertical plate was studied by England and Emery [19]. Elsaid and Abdel-wahed [20] have investigated MHD mixed convection Ferro Fe_3O_4/Cu-hybrid-nanofluid runs in a vertical channel. Kumar *et al.,* [21] developed a model to simulate the flow and heat transfer of a nanofluid across an infinite vertical plate subject to a magnetic field and viscous dissipation. Subsequent research by Ali *et al.,* [22] studied how thermal radiation made an impact on the MHD hybrid nanofluid flow along the stretching cylinder. In a situation where the bottom plate was permeable and stretchy, Lv *et al.,* [23] have investigated the impact of thermal radiation, hall current, and uneven heat source/sink on the flow of nanofluid between two horizontal flat plates. Rao and Deka [24] have considered the effect of thermal radiation and chemical reaction on MHD Casson nanofluid flow caused due to a stretching sheet. Very recently, Rao and Deka [25] made a numerical investigation on the heat and mass transfer phenomena of a nanofluid under the impact of solar radiation. Consider a rotating fluid that is steady–laminar–incompressible and has a constant angular velocity and contains electrically conducting Fe_3O_4/Al_2O_3 hybrid nanoparticles traveling at a uniform velocity $U_w=b_x$ over a stretched plate.

The Hall current effect is the direct result of the Lorentz force. The Lorentz force is that which governs the behavior of charged particles in a magnetic field. It is this force which accounts for the deflection of electron beams in magnetically deflected cathode ray tubes and the rotation of electric motor armatures. Early applications using the Hall effect were restricted to the laboratory because the output voltage obtainable from the then-available materials was too low to be of much practical use. With the advent of semiconductors, however, several new materials became readily available which have high charge mobilities, making them suitable for the manufacture of commercially feasible Hall devices. Kodi *et al.,* [26] have studied unsteady magneto-hydro-dynamics flow of Jeffrey fluid through porous media with thermal radiation, Hall current and Soret effects. Kodi *et al.,* [27] have reviewed processing to pass unsteady MHD flow of a second-grade fluid through a porous medium in the presence of radiation absorption exhibits Diffusion thermo, hall and ion slip effects. Suresh Kumar *et al.,* [28] have possessed Numerical analysis of magnetohydrodynamics Casson nanofluid flow with activation energy, Hall current and thermal radiation. Bafakeeh *et al.,* [29] have expressed Hall Current and Soret Effects on Unsteady MHD Rotating Flow of Second-Grade Fluid through Porous Media under the Influences of Thermal Radiation and Chemical Reactions. Deepthi *et al.,* [30] have reviewed Recent Development of Heat and Mass Transport in the Presence of Hall, Ion Slip and Thermo Diffusion in Radiative Second Grade Material: Application of Micromachines. Ganjikunta *et al.,* [31] have analyzed an unsteady MHD flow of a second-grade fluid passing through a porous medium in the presence of radiation absorption exhibits Hall and ion slip effects. Raghunath and Mohanaramana [32] have discussed Hall, Soret, and rotational effects on unsteady MHD rotating flow of a second-grade fluid through a porous medium in the presence of chemical reaction and aligned magnetic field. Kodi *et al.,* [33] have discussed Hall and ion slip radiative flow of chemically reactive second grade through porous saturated space via perturbation approach. Vaddemani *et al.,* [34] have possessed Effects of Hall Current, Activation Energy and Diffusion Thermo of MHD Darcy-Forchheimer Casson Nanofluid Flow in the Presence of Brownian Motion and Thermophoresis.

The main objective of this research is to examine the steady flow of laminar, incompressible, hybrid nanofluid above a stretchy, rotating plate with a hall current, Joule heating and chemical reaction using hybrid nanoparticles $Fe_3O_4/Al2O_3$ under the influence of a magnetic field. The fluid and plates are rotating simultaneously with constant speed about the axis of rotation. The governing equations of momentum, energy and concentration are transformed into ODEs by a similarity

transformation and tackled at MATLAB using the boundary value problem technique. The influence of different constraints is discussed in the form of graphs and tables.

2. Non-Newtonian Casson Fluid Model

To create the governing equations for Casson fluid flow when it is compressed between two parallel plates, the rheological equation shown below is employed [35].

$$\tau_{ij} = \begin{cases} 2\left(\mu_B + \dfrac{P_y}{\sqrt{2\pi}}\right) e_{ij}, \pi > \pi_{c,} \\ 2\left(\mu_B + \dfrac{P_y}{\sqrt{2\pi_C}}\right) e_{ij}, \pi < \pi_{c,} \end{cases} \tag{1}$$

In Eq. (1), $\pi = e_{ij}, e_{ij}$, Where e_{ij} are the $(i, j)\,th$ Component of the deformation rate, π is the product of the deformation rate with itself, π_C is a critical value of this product based on the non-Newtonian model, μ_B is the plastic dynamic viscosity of the non-Newtonian fluid and P_y the yield stress of the fluid.

$$P_y = \frac{\mu_B \sqrt{2\pi}}{\beta} \tag{2}$$

Denote the yield stress of fluid. Some fluids require a gradually increasing shear stress to maintain a constant strain rate and are called Rheopectic, in the case of Casson fluid (Non-Newtonian) flow where $\pi > \pi_c$

$$\mu = \mu_B + \frac{p_y}{\sqrt{2\pi}} \tag{3}$$

When Eq. (2) is substituted into Eq. (3), the kinematic viscosity may be expressed as

$$\vartheta = \frac{\mu}{\rho} = \frac{\mu_B}{\rho}\left(1 + \frac{1}{\beta}\right) \tag{4}$$

where $\beta = \dfrac{\mu_B \sqrt{2\pi_c}}{p_y}$ denotes the Casson fluid parameter. The nature of Non-Newtonian fluid vanishes and it behaves as Newtonian fluid when $\beta \to \infty$.

3. Flow Governing Equations

Consider a rotating fluid that is steady–laminar– incompressible and has a constant angular velocity and contains electrically conducting Fe_3O_4/Al_2O_3 hybrid nanoparticles traveling at a uniform velocity $U_w = b_x$ over a stretched plate. Nonlinear thermal radiation with heat flux $q_r = \dfrac{-4\sigma^*}{3\alpha^*}\left(\dfrac{\partial T^4}{\partial z}\right)$, uniform magnetic fields of intensity B_0 and hall current are applied to the plate in a normal direction.

The temperature on the surface is T_w, whereas T_∞ is the temperature away from the surface. The geometry of the problem is shown in Figure 1.

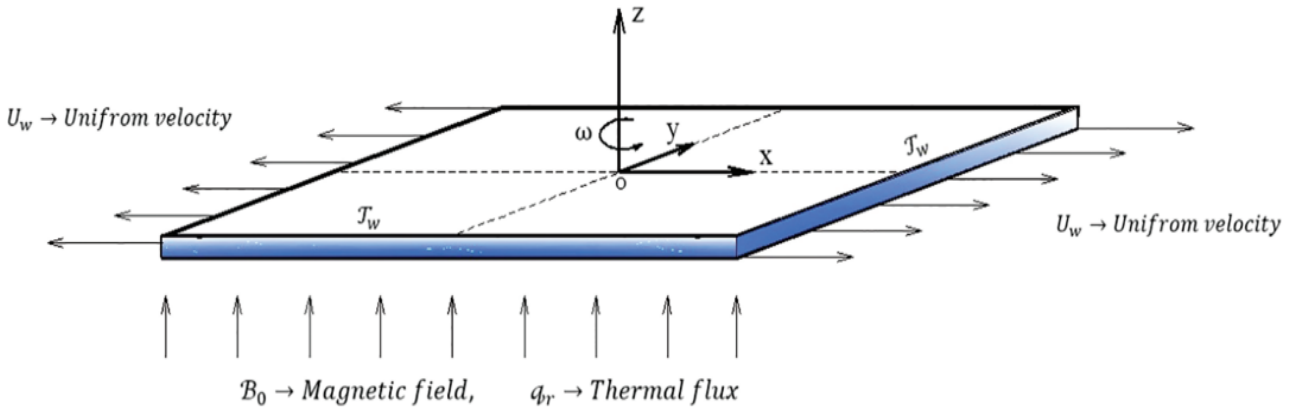

Fig. 1. The physical configuration of the problem

The equations describing the model are [18]:

$$\frac{\partial u}{\partial x}+\frac{\partial v}{\partial y}+\frac{\partial w}{\partial z}=0 \tag{5}$$

$$\rho_{hnf}\left(u\frac{\partial u}{\partial x}+v\frac{\partial u}{\partial y}+w\frac{\partial u}{\partial z}-2\omega v\right)=\mu_{hnf}\left(1+\frac{1}{\beta}\right)\frac{\partial^2 u}{\partial z^2}-\frac{\sigma_{hnf}B_0^2}{\left(1+m^2\right)}\left(u-mv\right) \tag{6}$$

$$\rho_{hnf}\left(u\frac{\partial v}{\partial x}+v\frac{\partial v}{\partial y}+w\frac{\partial v}{\partial z}+2\omega u\right)=\mu_{hnf}\left(1+\frac{1}{\beta}\right)\frac{\partial^2 v}{\partial z^2}-\frac{\sigma_{hnf}B_0^2}{\left(1+m^2\right)}\left(v+mu\right) \tag{7}$$

$$\left(\rho c_p\right)_{hnf}\left(u\frac{\partial T}{\partial x}+v\frac{\partial T}{\partial y}+w\frac{\partial T}{\partial z}\right)=k_{hnf}\left(\frac{\partial^2 T}{\partial z^2}\right)+\frac{\partial^2 T^4}{\partial z^2}\left(\frac{4\sigma^*}{3\alpha^*}\right)+\sigma_{hnf}B_0^2\left(u^2+v^2\right) \tag{8}$$

$$u\frac{\partial C}{\partial x}+v\frac{\partial C}{\partial y}+w\frac{\partial C}{\partial z}=\beta_{hnf}\left(\frac{\partial^2 C}{\partial z^2}\right)-k_r^2\left(C-C_\infty\right)\left(\frac{T}{T_\infty}\right)^m\exp\left(\frac{-E_a}{K^*T}\right) \tag{9}$$

For this flow, corresponding boundary conditions are for the governing PDEs are [18]

$$\begin{aligned} &u=U_w,\quad v=0,\quad w=0,\quad T=T_w,\quad C=C_w \quad \text{at } z=0,\\ &u\to 0,\quad v\to 0,\quad T\to T_\infty \quad C\to C_\infty \quad \text{as} \quad z\to\infty. \end{aligned} \tag{10}$$

The effective properties of hybrid nanofluid are given [18,20]:

$$\frac{\mu_{hnf}}{\mu_f}=\left(\frac{1}{\left(1-\phi_1\right)^{2.5}\left(1-\phi_2\right)^{2.5}}\right),$$

$$\rho_{hnf} = (1-\phi_2)\left[(1-\phi_2)\rho_f + \phi\rho_{s1}\right] + \phi_2\rho_{s2},$$

$$(\rho C_p)_{hnf} = (1-\phi_2)\left[(1-\phi_2)(\rho C_p)_f + \phi_1(\rho C_p)_{s1}\right] + \phi_2(\rho C_p)_{s2},$$

$$k_{nf} = k_f\left(\frac{k_{s1}+2k_{nf}-2\phi_1(k_{nf}-2k_{s1})}{k_{s1}+2k_{nf}+2\phi_1(k_{nf}-2k_{s1})}\right),$$

$$k_{hnf} = k_{nf}\left(\frac{k_{s2}+2k_{nf}-2\phi_2(k_{nf}-2k_{s2})}{k_{s2}+2k_{nf}+2\phi_2(k_{nf}-2k_{s2})}\right),$$

$$\sigma_{nf} = \sigma_f\left(\frac{\sigma_{s1}+2\sigma_{nf}-2\phi_1(\sigma_{nf}-2\sigma_{s1})}{\sigma_{s1}+2\sigma_{nf}+2\phi_1(\sigma_{nf}-2\sigma_{s1})}\right),$$

$$\sigma_{hnf} = \sigma_{nf}\left(\frac{\sigma_{s2}+2\sigma_{nf}-2\phi_2(\sigma_{nf}-2\sigma_{s2})}{\sigma_{s2}+2\sigma_{nf}+2\phi_2(\sigma_{nf}-2\sigma_{s2})}\right).$$

Here ϕ_1, $\phi 2$ are the solid volume fractions of Fe_3O_4 and Al_2O_3 respectively, subscript s_1, s_2, f, and h_{nf} are for nano-solid-particles, base fluid, and hybrid nanofluid respectively, as shown in Table 1.

Table 1
Thermo-physical properties of H_2O, Fe_3O_4, and Al_2O_3 [18,20]

Physical properties	Water	Fe_3O_4	Al_2O_3
C_p (J/KgK)	4179	670	765
ρ (Kg/m^3)	997.1	5180	3970
k (w/mK)	0.613	9.7	40
σ(Ω/m)	25*10^{-2}	25*10^3	35*10^6

Dimensionless quantities are introduced to simplify the mathematical analysis of the problem by introducing the following similarity transformation used to transform the PDEs to dimensionless ODEs

$$u = bx\,f'(\eta),\ v = by\,g(\eta),\ w = -\sqrt{b\nu_f}\,(f(\eta)+g(\eta)),\ T = T_\infty + \Delta T\,\theta(\eta),\quad \eta = \sqrt{\frac{b}{\nu_f}}z,\quad \theta(\eta) = \frac{T-T_\infty}{T_w-T_\infty},$$

$$\phi(\eta) = \frac{C-C_\infty}{C_w-C_\infty} \tag{11}$$

Substituting Eq. (11) into Eq. (6) to Eq. (9), we get the following system of non-linear ordinary differential equations

$$\left(\frac{l_4}{l_1}\right)\left(1+\frac{1}{\beta}\right)f''' - f'^2 + ff'' + 2\lambda g - \left(\frac{l_5}{l_1}\right)\frac{M}{(1+m^2)}(f'-mg) = 0 \tag{12}$$

$$\left(\frac{l_4}{l_1}\right)\left(1+\frac{1}{\beta}\right)g''+fg'-f'g-2\lambda f'-\left(\frac{l_5}{l_1}\right)\frac{M}{\left(1+m^2\right)}\left(g+mf'\right)=0 \tag{13}$$

$$\theta''+\left(\frac{R_d}{l_3}\right)\left[\left(1+\left(\theta_w-1\right)\theta\right)\right]^3\theta''+\Pr\left(\frac{l_2}{l_3}\right)f\theta'+\left(\frac{3R_d}{l_3}\right)\times\left(\theta_w-1\right)\left[\left(1+\left(\theta_w-1\right)\theta\right)\right]^2\theta'^2+\Pr Ec M\left(\frac{l_5}{l_3}\right)\times\left(f'^2+g'^2\right)=0 \tag{14}$$

$$\phi''+\frac{Sc}{\left(1-\phi_1\right)\left(1-\phi_2\right)}\left(f+g\right)\phi'-K_E\left(1+\theta\right)^m\varphi\exp\left(\frac{-E}{1+\theta}\right)=0 \tag{15}$$

Where the prime signifies differentiation with respect to (η) and it is given by ϕ2

$$l_1=\frac{\rho_{hnf}}{\rho_f},\ l_2=\frac{\left(\rho C_p\right)_{hnf}}{\left(\rho C_p\right)_f},\ l_3=\frac{k_{hnf}}{k_f},\ l_4=\frac{\mu_{hnf}}{\mu_f},\text{ and }\ l_5=\frac{\sigma_{hnf}}{\sigma_f}.$$

The transformed corresponding boundary conditions (10) become

$$\begin{aligned} &f(\eta)=0,\ \ g(\eta)=0,\ \ f'(\eta)=\theta,\ \ \theta(\eta)=1,\ \ \phi(\eta)=1 \qquad at \quad \eta=0,\\ &f'(\eta)\to 0,\ \ g(\eta)\to 0,\ \ \theta(\eta)\to 0,\ \ \phi(\eta)\to 0 \qquad as \quad \eta\to\infty. \end{aligned} \tag{16}$$

where prime denotes differentiation with respect to η, and the significant thermophysical parameters indicating the flow dynamics are defined by

$$\begin{cases} \lambda=\dfrac{\omega}{b}, M=\dfrac{\sigma_f B_0^2 x}{\rho_f b},\ \Pr=\dfrac{\nu_f}{k_f}=\dfrac{\left(\nu\rho C_p\right)_f}{k_f},\ \theta_w=\dfrac{T_w}{T_\infty},\ \ E_c=\dfrac{u^2\rho_f}{\left(\rho C_p\right)_f\left(T_w-T_\infty\right)}, \\ R_d=\dfrac{16\sigma^* T_\infty^3}{3k_f\alpha^*},\ S_c=\dfrac{\nu_f}{\beta_f}, K_E=\dfrac{k_r^2}{c}, E=\dfrac{E_a}{K^* T_\infty}, \delta=\dfrac{\left(T_w-T_\infty\right)}{T_\infty}. \end{cases} \tag{17}$$

4. Physical Quantities of Interests

The physical quantities of the given problem are, the ‘‘Skin friction” along x and y axis Cf_x; Cf_y, the ‘‘local Nusselt number” Nu_x and the ‘‘Sherwood number” Sh_x, defined by

$$Cf_x=\frac{\mu_{hnf}}{\rho_f\left(bx\right)^2}\left(\frac{\partial u}{\partial z}\right)_{z=0},\ \ Cf\ =\frac{\mu_{hnf}}{\rho_f\left(bx\right)^2}\left(\frac{\partial v}{\partial z}\right)_{z=0},$$
$$Nu_x=-\frac{xk_{hnf}}{k_f\left(T_w-T_\infty\right)}\left(\frac{\partial T}{\partial z}\right)_{z=0},\ Sh_x=-\frac{xk_{hnf}}{k_f\left(C_w-C_\infty\right)}\left(\frac{\partial C}{\partial z}\right)_{z=0} \tag{18}$$

The coefficient of skin friction, the Nusselt number, and the Sherwood number are all expressed in their non-dimensional versions in terms of the similarity variable as follows:

$$\mathrm{Re}_x^{1/2}\, Cf_x = \frac{\mu_{hnf}}{\mu_f} f''(0),\ \mathrm{Re}_x^{1/2}\, Cf_y = \frac{\mu_{hnf}}{\mu_f} g''(0),$$
$$\mathrm{Re}_x^{-1/2}\, Nu_x = -\left(\frac{k_{hnf}}{k_f} + Rd\theta_w^3\right)\theta'(0),\ \ \mathrm{Re}_x^{-1/2}\, Sh_x = -\frac{k_{hnf}}{k_f}\phi'(0) \tag{19}$$

5. Method of Solution

The set of non-linear coupled ordinary differential equations (12)-(15) have been solved numerically by RungeKutta-4th order method with shooting technique using MATLAB software with step size of $\nabla\eta$=0.01 and error bound 10^{-6} in all cases. Advantages of this method are that the coupled nonlinear ODEs are transformed to a set of linear first order ODEs with the introduction of the new variables. Secondly, the boundary value problem gets transformed to initial value problem by providing guess values to unknown initial values as required by the problem to be solved. The guess values are corrected by the shooting method to tally with the specified boundary conditions at the other boundary. Once the guess values are corrected with required number of iterations, then the forward integration is carried out to give the numerical solutions of the desired points comprising interval. The limitations are: Not all the PDEs, representing the governing equations, do not admit similarity transformations and cannot be transformed to ODEs. Only specific types of flow problems admit similarity transformations and hence similar solutions. There might be dual solutions to a specific problem, if exists, then which one is stable or unstable that is to be decided upon and discussed. To assess the accuracy of the present code and validity check, the numerical values of $f''(0), g'(0)$ and $Nu\, R_e^{-1/2}$ are presented in Table 2 and Table 3. Finally, the numerical simulations for the rate coefficients such as the shear rate, and heat transfer rate is obtained and exhibited in Table 4 for the variation of several contributing parameters. It is detected that the augmented values of the nanoparticle concentration, magnetic parameter, and thermal buoyancy enrich the rate of shear stress significantly. Further, the nanoparticle concentrations of both the Fe_3O_4 and Al_2O_3 increase the rate of heat transfer in magnitude whereas the other contributing parameters have retarding effect on the profile of the rate of heat transfer.

Table 2
Comparison of $f''(0), g'(0)$ with a previous studied when M=m=Ec=ϕ_1 =ϕ_2=Sc E=K_E=0

Elsaid and AlShurafat [18]			Current Study	
Λ	$f''(0)$	$g'(0)$	$f''(0)$	$g'(0)$
0.50	-1.13838	-0.51276	-1.14575	-0.509785
1.00	-1.32503	-0.83710	-1.32457	-0.834578
2.00	-1.65235	-1.28726	-1.64578	-1.277857

Table 3

Comparison of $Nu\,R_e^{-1/2}$ with a previous studied when M=1, Ec=0, ϕ_1=0.1, ϕ_2=0, λ =0.5, Sc=E=K_E=0

R_d	θ_w	Elsaid and AlShurafat [18]	Current Study
0	1	1.85750	1.86785
1	1	2.23679	2.23478
1	1.1	2.30471	2.31147
1	1.5	2.60865	2.60045

Table 4

Significant behaviour of the parameters on the rate coefficients

Φ_1	Φ_2	M	m	Ec	R_d	C_{fx}	C_{fy}	Nu_x
0	0.01	0	0	0	0	-0.9863	1.2341	1.2781
0.1						-0.9913	1.7323	1.3123
0.2						-1.0192	1.9621	1.4123
	0.1					-1.2524	1.6120	1.7652
	0.2					-0.9872	1.2412	1.6734
		0.1				-0.1262	1.6654	1.7562
		0.2				-0.9815	1.7773	1.6578
			0.2			-0.8223	1.2673	1.6674
			0.4			-0.9918	1.5723	1.5673
				0.2		-0.2712	1.5125	1.7129
				0.4		-0.7475	1.6621	1.4562
					0.2	-0.8948	1.5128	1.9695
					0.2	-0.6341	1.4624	0.9946

6. Results and Discussion

Over a stretched plate, a boundary layer is modeled over a rotating hybrid nanofluid with water as a base fluid and Fe_3O_4/Al_2O_3 nanoparticles. Through a series of Figure 3 to 6, effects magnetic field, hall current, rotation parameter, joule heating and nonlinear thermal radiation, on the boundary layer was investigated. Longitudinal velocity is measured along the x-axis, while transversal velocity is measured along the y-axis. In addition, Table 4 shows the influence of all employed parameters on heat flow and skin friction. The results will be discussed in the following section.

In Figure 2, the impact of magnetic field is indicated by the Hartman number (M), and it can be seen that rising the Hartman number reduces the velocities in x and y directions. Physically, introducing a magnetic field thins the boundary layer, reducing the fluid's ability to move in each direction. The existence of hall current alongside the magnetic field, furthermore, is indicated by a dashed line in each illustration. Certainly, the Hall current had no discernible impact on longitudinal velocity; however, the transversal velocity increased when the Hall current was present. Furthermore, as seen in Figure 3, the increase in transversal velocity is more visible when the magnetic strength is high. From a physical point of view, the existence of hall current under the influence of a magnetic field causes a drag perpendicular force known as a Lorentz force. As a result, one can see that this force causes the fluid molecules to shift their travel direction, resulting in an increase in transversal velocity. The impact of a magnetic field on temperature profiles is demonstrated in Figure 4, where the existence of a magnetic field causes fluid molecules near the surface to move, raising the boundary layer temperature. In addition, Due to influence of joule heating caused by the powerful magnetic field, the existence of hall current raises the thermal boundary layer thickness and the temperature of boundary layer.

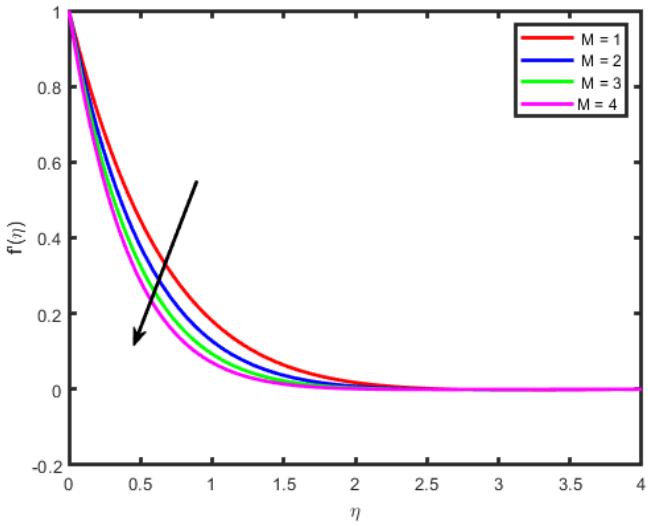

Fig. 2. Effect of M (weak magnetic strength) on $f'(\eta)$

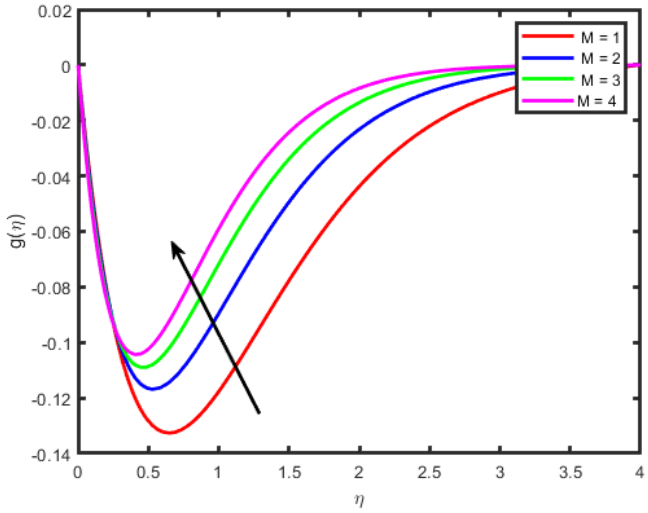

Fig. 3. Effect of M (weak magnetic strength) on $g(\eta)$

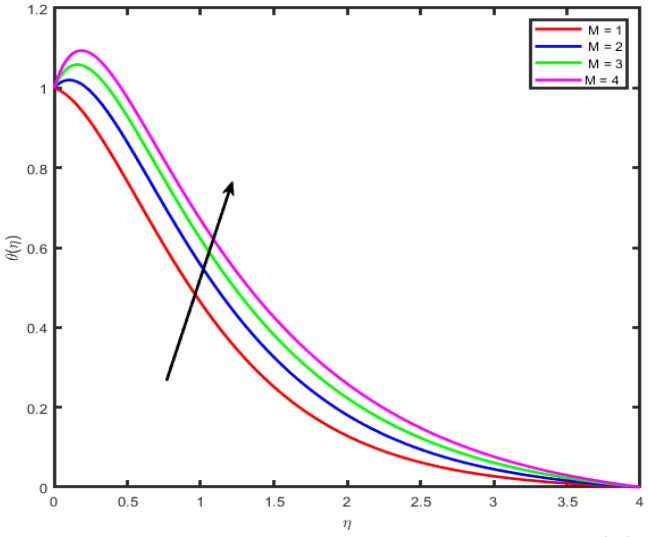

Fig. 4. Effect of M (weak magnetic strength) on $\theta(\eta)$

Figure 5 and 6 show the effects of Hall current parameter m on both longitudinal and transversal velocities profiles. Figure 5 illustrates that longitudinal velocity $f'(\eta)$ in fluid temperature enlarges due to increase of Hall current parameter m. Figure 6 shows the features of Hall parameter m on transversal velocity $g(\eta)$. It is observed that transversal velocity is a decreasing function of Hall parameter m.

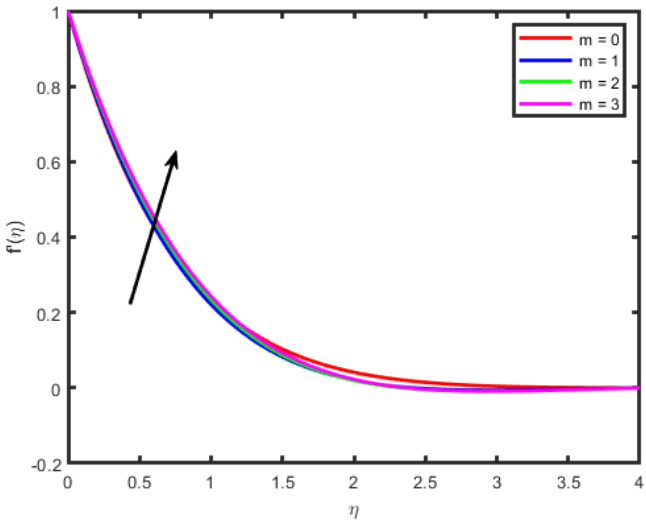

Fig. 5. Effect of m Hall parameter on $f'(\eta)$

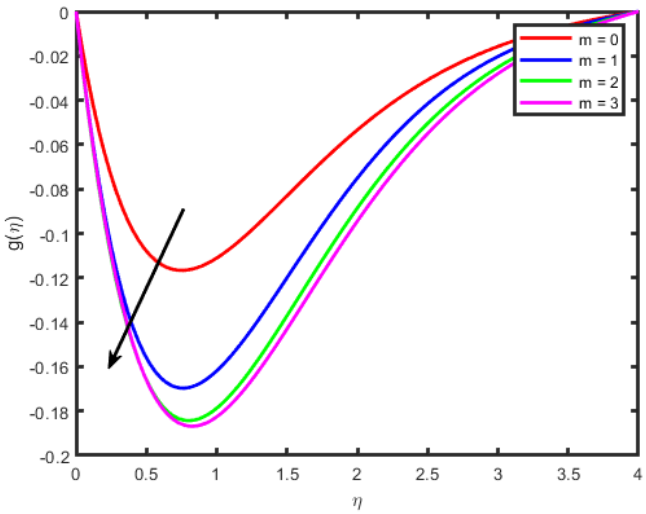

Fig. 6. Effect of m Hall parameter on $g(\eta)$

Figure 7 displays the effects of rotation parameter λ on longitudinal velocity $f'(\eta)$. The rotation parameter is defined as Ω\b. Thus, it clearly shows that increasing value of longitudinal velocity implies the strong rotation rate and therefore the rotation rate becomes higher as compared to the stretching rate. Physically, it is noted that an increase in rotation parameter implies boosting of the centrifugal force which in turns exerts pressure on the fluid to accelerate the fluid particles more rapidly in the radial direction. Similarly, the effects of rotation parameter λ on longitudinal velocity $g(\eta)$ as shown in Figure 8 displays that an increase in the rotation parameter λ causes to enhance the transversal velocity. Figure 9 and Figure 10 depict the effects of rotation parameter λ on temperature and concentration field respectively. It is illustrated that the temperature of hybrid

nanofluid decreases by enhancing the rotation rate. The similar behavior has observed in concentration field.

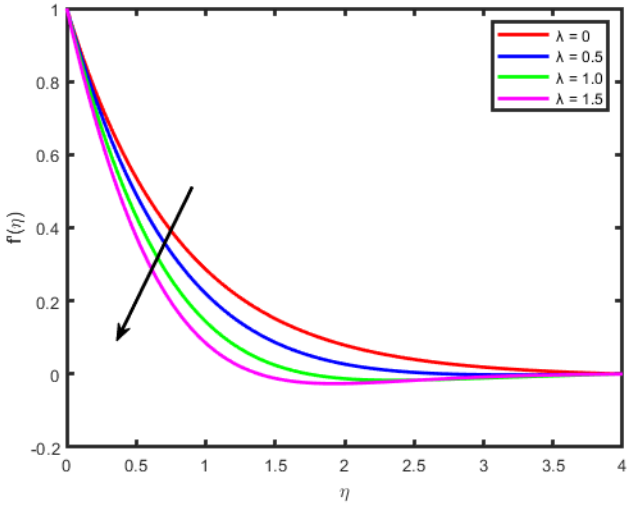

Fig. 7. Effect of λ Rotation parameter on $f'(\eta)$

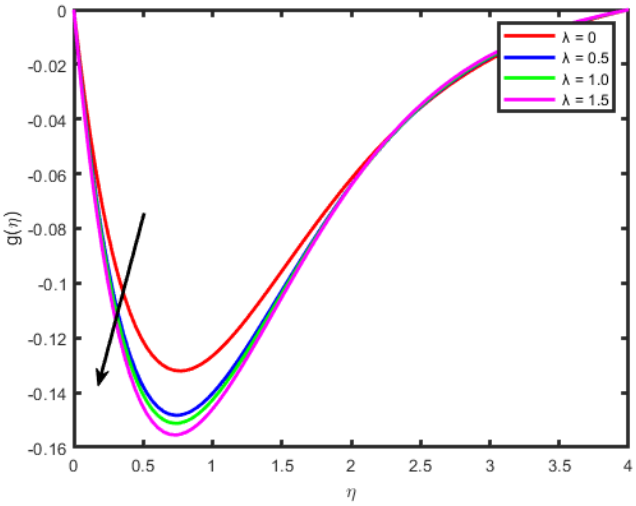

Fig. 8. Effect of λ Rotation parameter on $g(\eta)$

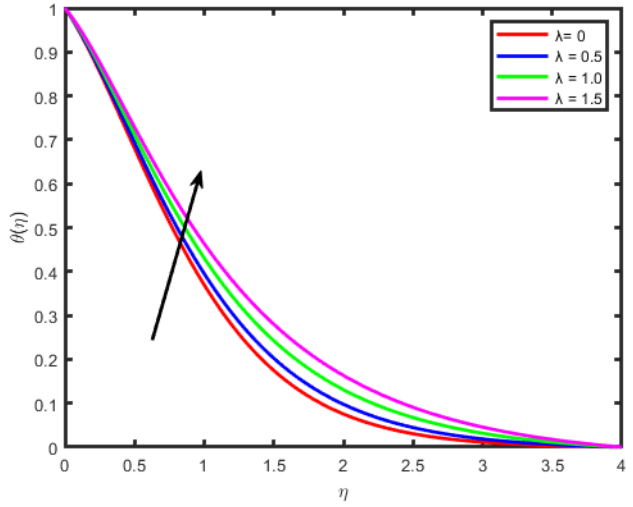

Fig. 9. Effect of λ Rotation parameter on $\theta(\eta)$

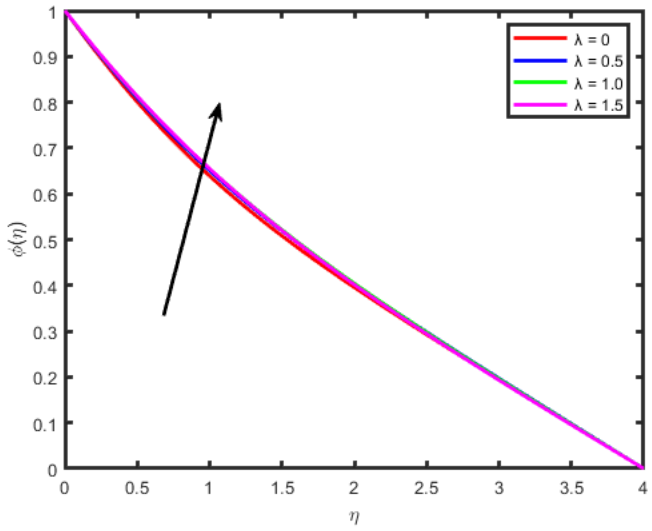

Fig. 10. Effect of λ Rotation parameter on $\phi(\eta)$

The impact of radiation parameter (Rd) on the temperature and concentration profile is shown in Figure 11 and 12. The figure shows the impact for both Fe_3O_4 and Al_2O_3 hybrid nanofluid it is evident that when the radiation parameter increases, the temperature rises. That's because what we are observing is the result of heat energy being released into the fluid as a result of an increase in thermal radiation. It is noteworthy to see that the hybrid nanofluid shows higher temperature profile than the ordinary nanofluid. The reversal behavior has observed in concentrate field.

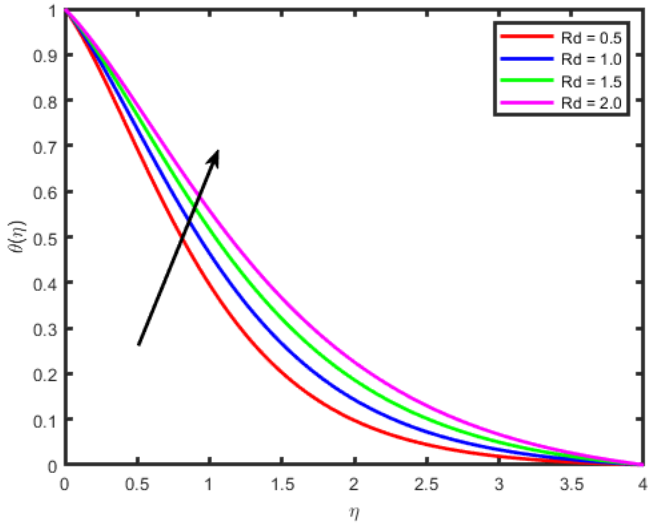

Fig. 11. Effect of R_d Radiation parameter on $\theta(\eta)$

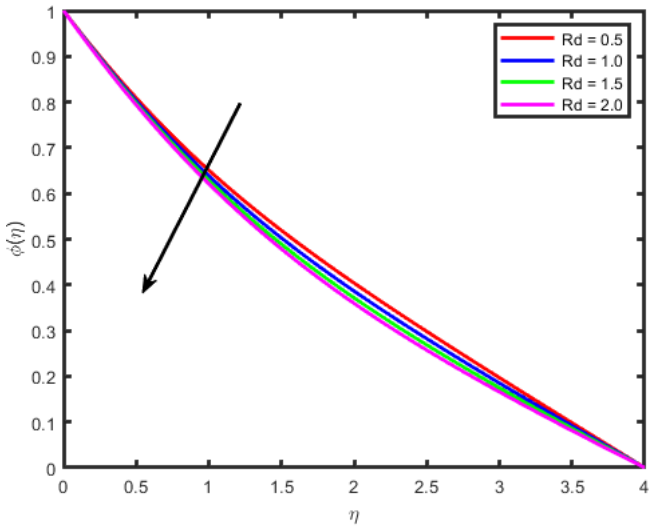

Fig. 12. Effect of R_d Radiation parameter on $\phi(\eta)$

Figure 13 and 14 show the influence of nanoparticle concentration on boundary layer velocity, showing that as the nanoparticles are used, the velocity decreases. Furthermore, utilizing a couple types of nanoparticles increases this decrease in velocity. Furthermore, the temperature and concentration profile rise, particularly in the form of a couple system of nanoparticles; this is caused by an increase in the mixing fluid's thermal conductivity, as seen in Figure 15 and 16. Figure 17 displays the effects of Eckert number Ec on the temperature field. The temperature field rises by increasing the amount of Eckert number. The reason behind is that the conversion of mechanical energy into thermal energy. This effect rises only due to heat dissipation.

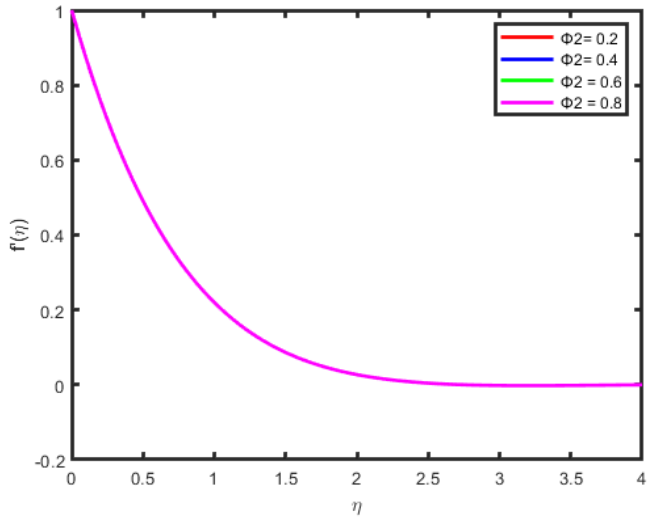

Fig. 13. Effect of ϕ_2 nanoparticle volume fraction on $f'(\eta)$

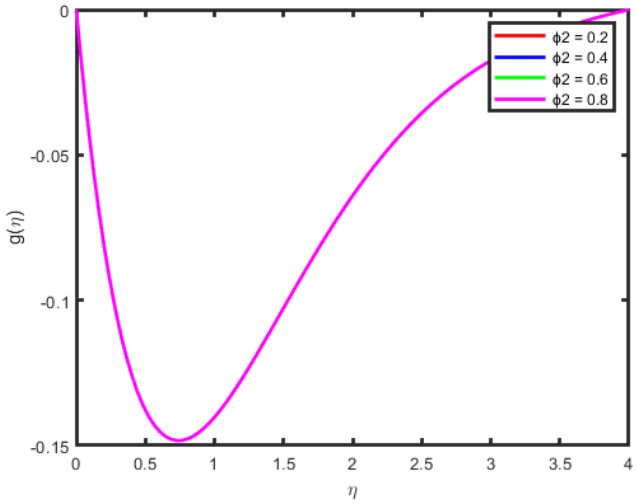

Fig. 14. Effect of ϕ_2 nanoparticle volume fraction on $g(\eta)$

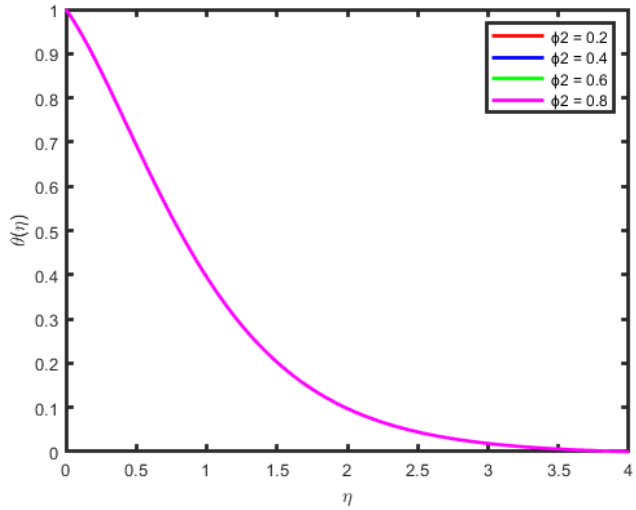

Fig. 15. Effect of ϕ_2 nanoparticle volume fraction on $\theta(\eta)$

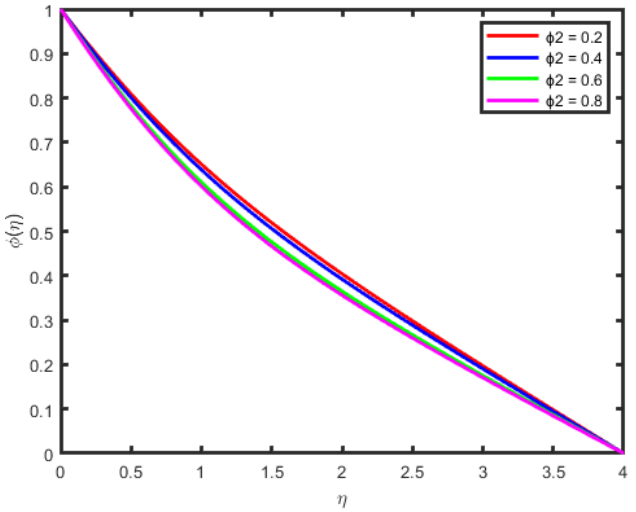

Fig. 16. Effect of ϕ_2 nanoparticle volume fraction on $\phi(\eta)$

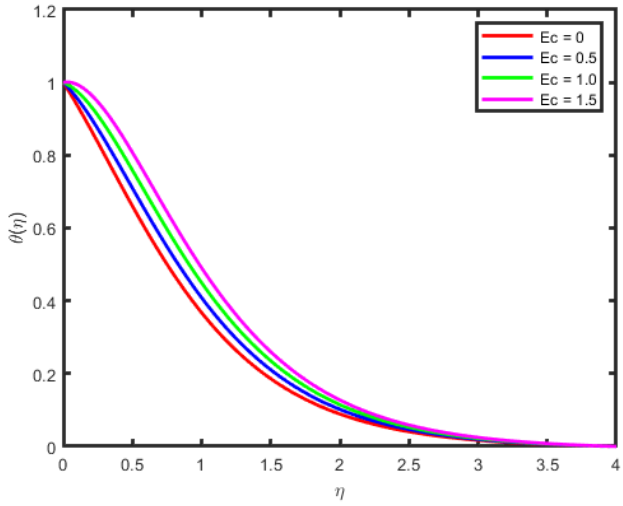

Fig. 17. Effect of E_c Eckert number on $\theta(\eta)$

Figure 18 envisages the activation energy (E) impact on concentration field. Graph elucidate that concentration profile increases for large value of E. The Arrhenius function deteriorations by snow balling the value of the activation energy, which outcomes in the promotion of the generative chemical reaction causing an improvement in the concentration field. Within the occurrence of low temperature and higher activation energy leads to a smaller reaction rate constant which slow down the chemical reaction. In this manner concentration profile boost up. Figure 19 shows that when chemical reaction rate (σ) increases, concentration profile strongly reduces because of high chemical reaction rate which fallouts solute boundary layer becomes thicker. When σ increases steadily, the factor $(1+\Gamma\theta)\ e^{-E/(1+\Gamma\theta)}$ is enriches because of increase in values σ. Figure 20 shows the effect of Schmidt number on concentration profile. It is a relation of momentum diffusivity and mass diffusivity. The concentration profile decays when the Schmidt number increases and a lower concentration boundary layer are noted for mixed nanoparticles hybrid nanofluid.

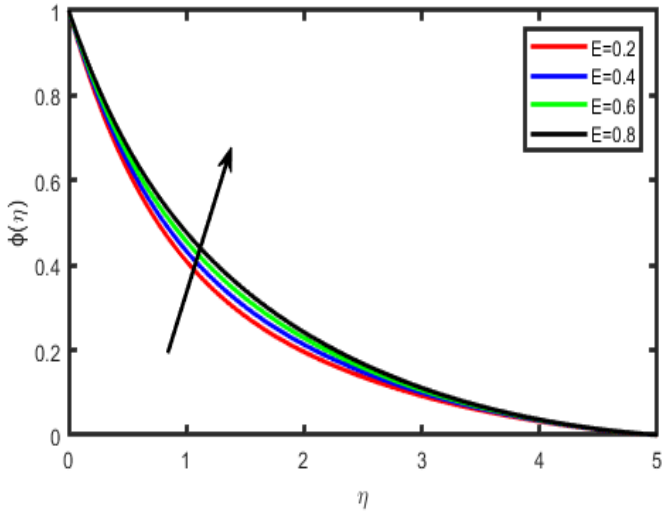

Fig. 18. Effect of Activation energy (E) on ϕ(η)

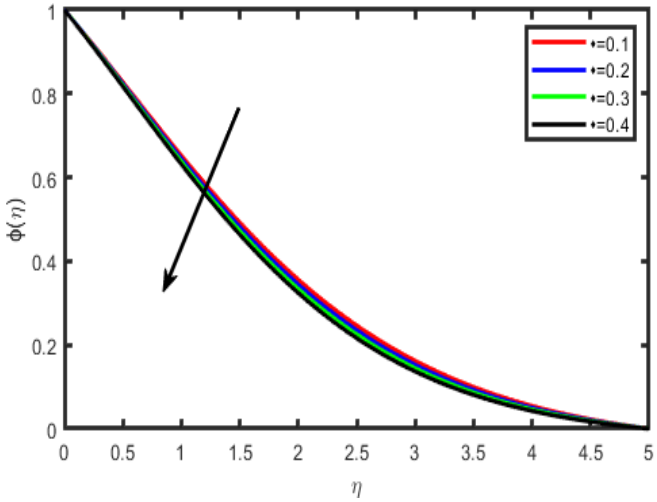

Fig. 19. Effect of chemical reaction rate (σ) on ϕ(η)

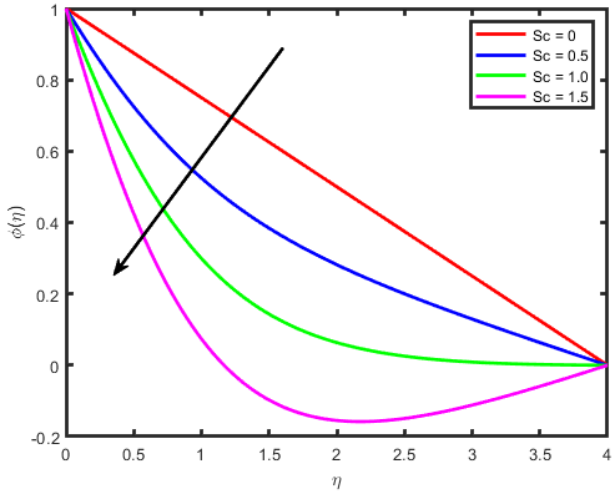

Fig. 20. Effect of S_C Schmidt number on $\phi(\eta)$

7. Conclusion

This work presented a mathematical simulation to study the impact of Hall current, magnetic field, joule heating, rotation parameter, and nonlinear thermal radiation on a rotating hybrid Fe_3O_4/Al_2O_3 nanofluid over-stretched plate using a set of governing partial differential equations. The system transformed to be dimensionless one dimension of a single variable and then solved numerically with a mix of find root and Runge Kutta method to overcome the missing of the boundary conditions. The following are the most important aspects of this research:

i. An increment in the magnetic parameter M diminishes the velocity of the hybrid nanofluid, but at the same time, causing enhances in the profile of (η), temperature and concentration of the hybrid nanofluid.
ii. When the rotation parameter is present the longitudinal velocity decreases while the transverse velocity increases and the temperature of a boundary layer rise as the kinetic energy of the fluid increases. When a boundary layer is exposed to thermal radiation, it has a higher temperature than when it isn't.
iii. Because the fluid viscosity rises when a dual-type of the nanoparticle is used, the velocity decreases more rapidly.

The propose study brings a road way to analyze the physical behaviour of the various nanoparticles on the hybrid nanofluid flow and their real-life applications in industries as well as engineering. In a broad sense, cooling is one of the important applications where the range of the temperature is high. For example, refrigeration as well as the ventilation, and air conditioning applications are commonly used.

References

[1] Choi, S. U. S., and Jeffrey A. Eastman. *Enhancing thermal conductivity of fluids with nanoparticles*. No. ANL/MSD/CP-84938; CONF-951135-29. Argonne National Lab.(ANL), Argonne, IL (United States), 1995.

[2] Buongiorno, Jacopo. "Convective transport in nanofluids." *ASME Journal of Heat and Mass Transfer* 128, no. 3 (2006): 240-250. https://doi.org/10.1115/1.2150834

[3] Nield, D. A., and Andrey V. Kuznetsov. "Thermal instability in a porous medium layer saturated by a nanofluid." *International Journal of Heat and Mass Transfer* 52, no. 25-26 (2009): 5796-5801. https://doi.org/10.1016/j.ijheatmasstransfer.2009.07.023

[4] Khan, W. A., and I. Pop. "Boundary-layer flow of a nanofluid past a stretching sheet." *International Journal of Heat and Mass Transfer* 53, no. 11-12 (2010): 2477-2483. https://doi.org/10.1016/j.ijheatmasstransfer.2010.01.032

[5] Hamid, Aamir, M. Ijaz Khan, R. Naveen Kumar, R. J. Punith Gowda, and B. C. Prasannakumara. "Numerical study of bio-convection flow of magneto-cross nanofluid containing gyrotactic microorganisms with effective Prandtl number approach." *Science Reports* (2021). https://doi.org/10.21203/rs.3.rs-435508/v1

[6] Varun Kumar, R. S., A. Alhadhrami, R. J. Punith Gowda, R. Naveen Kumar, and B. C. Prasannakumara. "Exploration of Arrhenius activation energy on hybrid nanofluid flow over a curved stretchable surface." *ZAMM-Journal of Applied Mathematics and Mechanics/Zeitschrift für Angewandte Mathematik und Mechanik* 101, no. 12 (2021): e202100035. https://doi.org/10.1002/zamm.202100035

[7] Shah, Syed Asif Ali, N. Ameer Ahammad, ElSayed M. Tag El Din, Fehmi Gamaoun, Aziz Ullah Awan, and Bagh Ali. "Bio-convection effects on prandtl hybrid nanofluid flow with chemical reaction and motile microorganism over a stretching sheet." *Nanomaterials* 12, no. 13 (2022): 2174. https://doi.org/10.3390/nano12132174

[8] Faraz, Faraz, Syed Muhammad Imran, Bagh Ali, and Sajjad Haider. "Thermo-diffusion and multi-slip effect on an axisymmetric Casson flow over a unsteady radially stretching sheet in the presence of chemical reaction." *Processes* 7, no. 11 (2019): 851. https://doi.org/10.3390/pr7110851

[9] Arshad, Mubashar, and Ali Hassan. "A numerical study on the hybrid nanofluid flow between a permeable rotating system." *The European Physical Journal Plus* 137, no. 10 (2022): 1126. https://doi.org/10.1140/epjp/s13360-022-03313-2

[10] Hassan, Ali, Azad Hussain, Mubashar Arshad, Soumaya Gouadria, Jan Awrejcewicz, Ahmed M. Galal, Fahad M. Alharbi, and S. Eswaramoorthi. "Insight into the significance of viscous dissipation and heat generation/absorption in magneto-hydrodynamic radiative casson fluid flow with first-order chemical reaction." *Frontiers in Physics* (2022): 605. https://doi.org/10.3389/fphy.2022.920372

[11] Krishnamurthy, M. R., B. J. Gireesha, B. C. Prasannakumara, and Rama Subba Reddy Gorla. "Thermal radiation and chemical reaction effects on boundary layer slip flow and melting heat transfer of nanofluid induced by a nonlinear stretching sheet." *Nonlinear Engineering* 5, no. 3 (2016): 147-159. https://doi.org/10.1515/nleng-2016-0013

[12] Sundar, L. Syam, Korada Viswanatha Sharma, Manoj K. Singh, and A. C. M. Sousa. "Hybrid nanofluids preparation, thermal properties, heat transfer and friction factor-a review." *Renewable and Sustainable Energy Reviews* 68 (2017): 185-198. https://doi.org/10.1016/j.rser.2016.09.108

[13] Waini, Iskandar, Anuar Ishak, and Ioan Pop. "Unsteady flow and heat transfer past a stretching/shrinking sheet in a hybrid nanofluid." *International Journal of Heat and Mass Transfer* 136 (2019): 288-297. https://doi.org/10.1016/j.ijheatmasstransfer.2019.02.101

[14] Lund, Liaquat Ali, Zurni Omar, Ilyas Khan, and El-Sayed M. Sherif. "Dual solutions and stability analysis of a hybrid nanofluid over a stretching/shrinking sheet executing MHD flow." *Symmetry* 12, no. 2 (2020): 276. https://doi.org/10.3390/sym12020276

[15] Shoaib, Muhammad, Muhammad Asif Zahoor Raja, Muhammad Touseef Sabir, Muhammad Awais, Saeed Islam, Zahir Shah, and Poom Kumam. "Numerical analysis of 3-D MHD hybrid nanofluid over a rotational disk in presence of thermal radiation with Joule heating and viscous dissipation effects using Lobatto IIIA technique." *Alexandria Engineering Journal* 60, no. 4 (2021): 3605-3619. https://doi.org/10.1016/j.aej.2021.02.015

[16] Ahmad, Farooq, Sohaib Abdal, Hela Ayed, Sajjad Hussain, Suleman Salim, and A. Othman Almatroud. "The improved thermal efficiency of Maxwell hybrid nanofluid comprising of graphene oxide plus silver/kerosene oil over

stretching sheet." *Case Studies in Thermal Engineering* 27 (2021): 101257. https://doi.org/10.1016/j.csite.2021.101257

[17] Alhussain, Ziyad A., and Asifa Tassaddiq. "Thin film blood based Casson hybrid nanofluid flow with variable viscosity." *Arabian Journal for Science and Engineering* 47, no. 1 (2022): 1087-1094. https://doi.org/10.1007/s13369-021-06067-8

[18] Elsaid, Essam M., and Khalid S. AlShurafat. "Impact of hall current and joule heating on a rotating hybrid nanofluid over a stretched plate with nonlinear thermal radiation." *Journal of Nanofluids* 12, no. 2 (2023): 548-556. https://doi.org/10.1166/jon.2023.1927

[19] England, W. G., and A. F. Emery. "Thermal radiation effects on the laminar free convection boundary layer of an absorbing gas." *ASME Journal of Heat and Mass Transfer* 91, no. 1 (1969): 37-44. https://doi.org/10.1115/1.3580116

[20] Elsaid, Essam M., and Mohamed S. Abdel-wahed. "MHD mixed convection Ferro Fe_3O_4/Cu-hybrid-nanofluid runs in a vertical channel." *Chinese Journal of Physics* 76 (2022): 269-282. https://doi.org/10.1016/j.cjph.2021.12.016

[21] Kumar, M. Anil, Y. Dharmendar Reddy, V. Srinivasa Rao, and B. Shankar Goud. "Thermal radiation impact on MHD heat transfer natural convective nano fluid flow over an impulsively started vertical plate." *Case Studies in Thermal Engineering* 24 (2021): 100826. https://doi.org/10.1016/j.csite.2020.100826

[22] Ali, Aamir, Tasmia Kanwal, Muhammad Awais, Zahir Shah, Poom Kumam, and Phatiphat Thounthong. "Impact of thermal radiation and non-uniform heat flux on MHD hybrid nanofluid along a stretching cylinder." *Scientific Reports* 11, no. 1 (2021): 20262. https://doi.org/10.1038/s41598-021-99800-0

[23] Lv, Yu-Pei, Naila Shaheen, Muhammad Ramzan, M. Mursaleen, Kottakkaran Sooppy Nisar, and M. Y. Malik. "Chemical reaction and thermal radiation impact on a nanofluid flow in a rotating channel with Hall current." *Scientific Reports* 11, no. 1 (2021): 19747. https://doi.org/10.1038/s41598-021-99214-y

[24] Rao, Shiva, and Paramananda Deka. "A numerical solution using EFDM for unsteady MHD radiative Casson nanofluid flow over a porous stretching sheet with stability analysis." *Heat Transfer* 51, no. 8 (2022): 8020-8042. https://doi.org/10.1002/htj.22679

[25] Rao, Shiva, and P. N. Deka. "A numerical investigation on transport phenomena in a nanofluid under the transverse magnetic field over a stretching plate associated with solar radiation." In *Nonlinear Dynamics and Applications: Proceedings of the ICNDA 2022*, pp. 473-492. Cham: Springer International Publishing, 2022. https://doi.org/10.1007/978-3-030-99792-2_39

[26] Raghunath, Kodi, Ramachandra Reddy Vaddemani, M. Ijaz Khan, Sherzod Shukhratovich Abdullaev, Attia Boudjemline, Mohamed Boujelbene, and Yassine Bouazzi. "Unsteady magneto-hydro-dynamics flow of Jeffrey fluid through porous media with thermal radiation, Hall current and Soret effects." *Journal of Magnetism and Magnetic Materials* 582 (2023): 171033. https://doi.org/10.1016/j.jmmm.2023.171033

[27] Raghunath, Kodi, Ravuri Mohana Ramana, Charankumar Ganteda, Prem Kumar Chaurasiya, Damodar Tiwari, Rajan Kumar, Dharam Buddhi, and Kuldeep Kumar Saxena. "Processing to pass unsteady MHD flow of a second-grade fluid through a porous medium in the presence of radiation absorption exhibits Diffusion thermo, hall and ion slip effects." *Advances in Materials and Processing Technologies* (2023): 1-18. https://doi.org/10.1080/2374068X.2023.2191450

[28] Suresh Kumar, Y., Shaik Hussain, K. Raghunath, Farhan Ali, Kamel Guedri, Sayed M. Eldin, and M. Ijaz Khan. "Numerical analysis of magnetohydrodynamics Casson nanofluid flow with activation energy, Hall current and thermal radiation." *Scientific Reports* 13, no. 1 (2023): 4021. https://doi.org/10.1038/s41598-023-28379-5

[29] Bafakeeh, Omar T., Kodi Raghunath, Farhan Ali, Muhammad Khalid, El Sayed Mohamed Tag-ElDin, Mowffaq Oreijah, Kamel Guedri, Nidhal Ben Khedher, and Muhammad Ijaz Khan. "Hall current and Soret effects on unsteady MHD rotating flow of second-grade fluid through porous media under the influences of thermal radiation and chemical reactions." *Catalysts* 12, no. 10 (2022): 1233. https://doi.org/10.3390/catal12101233

[30] Deepthi, V. V. L., Maha MA Lashin, N. Ravi Kumar, Kodi Raghunath, Farhan Ali, Mowffaq Oreijah, Kamel Guedri, El Sayed Mohamed Tag-ElDin, M. Ijaz Khan, and Ahmed M. Galal. "Recent development of heat and mass transport in the presence of Hall, ion slip and thermo diffusion in radiative second grade material: application of micromachines." *Micromachines* 13, no. 10 (2022): 1566. https://doi.org/10.3390/mi13101566

[31] Ganjikunta, Aruna, Hari Babu Kommaddi, Venkateswarlu Bhajanthri, and Raghunath Kodi. "An unsteady MHD flow of a second-grade fluid passing through a porous medium in the presence of radiation absorption exhibits Hall and ion slip effects." *Heat Transfer* 52, no. 1 (2023): 780-806. https://doi.org/10.1002/htj.22716

[32] Raghunath, Kodi, and Ravuri Mohanaramana. "Hall, Soret, and rotational effects on unsteady MHD rotating flow of a second-grade fluid through a porous medium in the presence of chemical reaction and aligned magnetic field." *International Communications in Heat and Mass Transfer* 137 (2022): 106287. https://doi.org/10.1016/j.icheatmasstransfer.2022.106287

[33] Kodi, Raghunath, Mohanaramana Ravuri, Nagesh Gulle, Charankumar Ganteda, Sami Ullah Khan, and M. Ijaz Khan. "Hall and ion slip radiative flow of chemically reactive second grade through porous saturated space via perturbation approach." *Waves in Random and Complex Media* (2022): 1-17. https://doi.org/10.1080/17455030.2022.2108555

[34] Vaddemani, Ramachandra Reddy, Sreedhar Ganta, and Raghunath Kodi. "Effects of Hall Current, Activation Energy and Diffusion Thermo of MHD Darcy-Forchheimer Casson Nanofluid Flow in the Presence of Brownian Motion and Thermophoresis." *Journal of Advanced Research in Fluid Mechanics and Thermal Sciences* 105, no. 2 (2023): 129-145. https://doi.org/10.37934/arfmts.105.2.129145

[35] Abdel-Wahed, Mohamed S. "Rotating ferro-nanofluid over stretching plate under the effect of hall current and joule heating." *Journal of Magnetism and Magnetic Materials* 429 (2017): 287-293. https://doi.org/10.1016/j.jmmm.2017.01.032